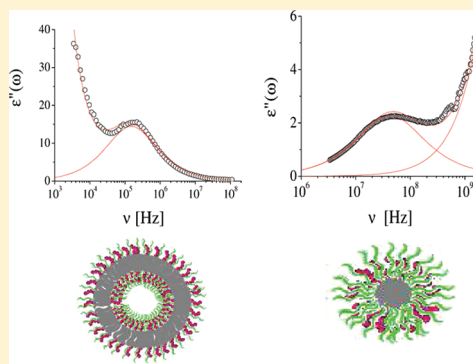


Assemblies of Thermoresponsive Diblock Copolymers: Micelle and Vesicle Formation Investigated by Means of Dielectric Relaxation Spectroscopy

G. Masci,[†] R. D. Ladogana,[†] and C. Cametti^{*,‡}

[†]Department of Chemistry, and [‡]Department of Physics and CNR-INFM-SOFT, "La Sapienza" University of Rome, Piazzale A. Moro 5, I-00185 Rome, Italy

ABSTRACT: The dielectric properties of aqueous solutions of two different thermoresponsive mixed copolymers, (3-acrylamidopropyl)-trimethylammonium chloride and *N*-isopropylacrylamide, PAMPTMA-*b*-NIPAAm, and sodium 2-acrylamido-2-methylpropanesulfonate and *N*-isopropylacrylamide, PAMPS-*b*-PNIPAAm, have been investigated in the frequency range where marked interfacial polarization mechanisms occur, both below and above the lower critical solution temperature. In the presence of poly(ethylene oxide)-PNIPAAm block polymers, PEO-*b*-PNIPAAm, these classes of copolymers give rise to different types of aggregates with different compositions and different architectures. By the combined results from dielectric relaxation spectroscopy, dynamic light scattering, and ζ -potential measurements, we give evidence for assembling into two different composite structures, a core-shell-type micellar structure built up by a hydrophobic core surrounded by a hydrophilic charged layer, in the case of the PEO-*b*-PNIPAAm + PAMPS-*b*-PNIPAAm system, and a vesicular structure encompassing an aqueous core in the case of the PEO-*b*-PNIPAAm + PAMPTMA-*b*-PNIPAAm system. These different structures, governed by a delicate interplay between electrostatic and hydrophobic interactions, are characterized by dielectric parameters (dielectric increments and relaxation frequencies) that can be properly deduced from suitable dielectric models, in the framework of heterogeneous system theory. These structures and in particular hollow particles with a large internal aqueous core, where large hydrophilic compounds can be encapsulated, offer novel and interesting properties in biomedical technologies and in particular in drug delivery as drug mesoscopic carriers.



1. INTRODUCTION

Amphiphilic block copolymers, where different blocks are connected by covalent bonds, have attracted a great deal of interest because of their temperature-induced self-assembly properties.^{1–3} These polymers, which are able to self-assemble into different morphologies, depending on external stimuli, such as pH, temperature, and ionic strength,⁴ give rise to structures that have a broad range of biotechnological applications,^{5–7} including drug delivery, encapsulation, adhesives, and compatibilizers.^{8–10}

Among them, poly(*N*-isopropylacrylamide) (PNIPAAm) is a widely investigated temperature-sensitive polymer which exhibits a lower critical solution temperature (LCST) at around 33–35 °C.¹¹ This behavior is due to the balance between hydrophilic and hydrophobic groups in the polymer chain. Below LCST, interactions of water molecules with hydrophilic segments of the chain make the polymer soluble in water,¹² whereas polymer–polymer interactions prevail above LCST and hydrophobic groups aggregate, making the polymer insoluble in water.¹³ This transition is related to a dehydration process occurring with a rearrangement of water molecules. The LCST phase transition of PNIPAAm is an endothermic process because of the disrupting of hydrogen bonds between water molecules and amide groups.¹⁴ These copolymers

undergo a micellization process consisting of supramolecular structures with a hydrophilic corona and a hydrophobic core.¹⁵ The dielectric properties of sodium 2-acrylamido-2-methylpropanesulfonate and *N*-isopropylacrylamide [PAMPS-*b*-PNIPAAm] polymer aqueous solutions have been recently investigated by us¹⁶ as a function of temperature with the aid of dielectric relaxation technique, and the resulting micellar structures above the LCST have been characterized in light of the standard electrokinetic model.

In this work, we have synthesized two different diblock copolymers, (3-acrylamidopropyl)trimethylammonium chloride and *N*-isopropylacrylamide, PAMPTMA-*b*-PNIPAAm, and sodium 2-acrylamido-2-methylpropanesulfonate and *N*-isopropylacrylamide, PAMPS-*b*-PNIPAAm, both of them known to self-assemble in aqueous media because of their thermosensitive nature.

We have investigated their behavior in the presence of PEO-*b*-PNIPAAm and have explored the association features of these two mixed systems by means of dielectric relaxation spectroscopy measurements, over an extended frequency range,

Received: December 14, 2011

Revised: January 25, 2012

Published: January 26, 2012

where the polarization mechanisms characteristic of highly heterogeneous systems take place, together with dynamic light scattering and electrophoretic mobility measurements, in order to characterize the hydrodynamic and electrical properties of the aggregates.

The structure of the polymers has been tailored in order to have, in the two different compositions, the hydrophobic blocks of approximately the same length ($n \simeq 100$). The hydrophilic blocks have a different polymerization degree ($n = 36$ and 30 for PAMPS and PAMPTMA, respectively, and $n = 114$ for PEO chains).

Each of the two block copolymers studied (i.e., PEO-*b*-PNIPAAM + PAMPTMA-*b*-PNIPAAM and PEO-*b*-PNIPAAM + PAMPS-*b*-PNIPAAM) exhibited a different behavior upon heating, ultimately resulting in the formation of aggregates having very different hydrodynamic diameters. In the former case, we are induced to hypothesize the formation of a thermosensitive symmetric hallow vesicle with a PNIPAAM hydrophobic shell covered on both sides with hydrophilic chains of PEO and PAMPTMA polymers. The hydrophilic blocks from the inner and outer hydrophobic shell produce an enhanced thermal stability of the vesicle. In the latter case, we are inclined to suppose the formation of a micellar structure whose core is formed by PNIPAAM polymers covered by a hydrophilic layer extending toward the outside formed by PEO and PAMPS polymers.

The two different morphological structures are sustained, besides results from dynamic light scattering measurements and by ζ -potential measurements, by the analysis of the dielectric relaxation processes we have observed on the basis of two different dielectric models, consisting of a hydrophobic core covered by a charged hydrophilic shell in the case of a micellar structure and of a hallow hydrophobic shell coated on both sides by charged hydrophilic polymeric chains in the case of a vesicular structure.

The two dielectric models we have employed, whose basic structures are schematically sketched in Figure 1, take explicitly

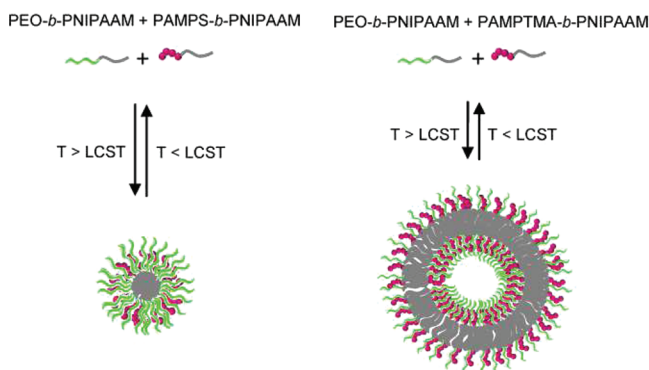


Figure 1. Sketch of the different structures formed by PEO-*b*-PNIPAAM + PAMPTMA-*b*-PNIPAAM and PEO-*b*-PNIPAAM + PAMPS-*b*-PNIPAAM polymer solutions upon temperature increase above LCST.

into account the charge distribution at the aqueous interfaces and, in the case of the vesicular structure, particularly at the inner interface.

The paper is organized as follows. In the next sections, after a brief description of the experimental setup employed, we present the dielectric spectra and preliminarily we discuss the phenomenological features that suggest different structural

organizations above the LCST in the two systems investigated. In section 5, we present in detail the two dielectric models employed, in light of the standard electrokinetic model for the micellar aggregates and in light of a recent model proposed by Prodan et al.¹⁷ for spherical biological cells for the vesicular aggregates, together with a discussion of the results. Section 8 contains some concluding remarks.

2. EXPERIMENTAL SECTION

2.1. Materials. The synthesis of PAMPS₃₆-*b*-PNIPAAM₉₆ and PAMPTMA₃₀-*b*-PNIPAAM₁₂₀ polymers (the numbers indicate the number average degree of polymerization X_n of polymer) by atom transfer radical polymerization (ATRP) has been already reported.^{18,19} PEO₁₁₄-*b*-PNIPAAM₁₀₀ has been synthesized by ATRP starting from a PEO macroinitiator prepared as already reported.²⁰ PNIPAAM was polymerized starting from the PEO macroinitiator as described in a previous paper.²¹ The polymer solutions, at the concentration of 5 mg/mL, were investigated at the ionic strength of 10^{-3} M NaCl, and the pH value was around 6.5.

2.2. Characterization of the Core–Shell Micelles and Vesicles. Particle size was measured by dynamic light scattering (DSL), and the particle surface electrical characterization was carried out by means of ζ -potential measurements.

2.2.1. Dynamic Light Scattering Measurements. Dynamic light scattering experiments were carried out, at the scattering angle of 90° , by means of a Brookhaven instrument equipped with a digital time correlator and with a He–Ne laser (output power 10 mW and wavelength of 632.8 nm) as the light source. The temperature of the thermostatted cell was varied from 10 to 50°C and controlled within 0.1°C . The experimentally recorded intensity autocorrelation function $g^2(q, t)$ is directly related to the first-order electric field autocorrelation function $g^1(q, t)$ through the Siegert relationship²² $g^2(q, t) = 1 + A|g^1(q, t)|^2$, where A is an instrumental parameter.

Depending on temperature, it could be expected that an aqueous solution of PAMPTMA-*b*-PNIPAAM or PAMPS-*b*-PNIPAAM copolymers contains progressively different type of species, starting from unimers, at lower temperature, up to micelles or intermicellar aggregates, at higher temperature. This different morphological evolution reflects in differently shaped correlation functions, which deviate from a single exponential decay as the temperature increases.

In the present case, the correlation function, at each temperature, can be described by a single stretched exponential

$$g^1(t) = A \exp[-(t/\tau_f)^\gamma] \quad (1)$$

where τ_f is the characteristic time and the exponent γ reflects deviations from a single exponential decay.

The apparent hydrodynamic radius R_H of the species present in the solution can be calculated by using the Stokes–Einstein relationship

$$R_H = \frac{K_B T}{6\pi\eta D} \quad (2)$$

where $K_B T$ is the thermal energy, η the viscosity of the solvent, and D the diffusion coefficient given by $D = 1/(\tau_f q^2)$. In the temperature interval investigated, the viscosity of the aqueous phase was assumed to be the one of water at the temperature of the experiment.

All experiments were carried out at a fixed polymer concentration of 5 mg/mL (dilute regime). To assess

polydispersity within each sample, the correlation functions were analyzed using the non-negative least-squares (NNLS)²³ or CONTIN²⁴ algorithms supplied with the instrument software. For all the sample investigated, the polydispersity *pdi*, defined as the second cumulant of the scattered light correlation function analyzed by the cumulant method divided by the average decay rate, was lower than *pdi* = 0.15.

The hydrodynamic diameter $2R_H$ of PEO₁₁₄-*b*-PNIPAAm₁₀₀ + PAMPTMA₃₀-*b*-NIPAAm₁₂₀ and PEO₁₁₄-*b*-PNIPAAm₁₀₀ + PAMPS₃₆-*b*-PNIPAAm₉₆ in aqueous suspension is shown in Figure 2, in the whole temperature range investigated, from 10 to 50 °C.

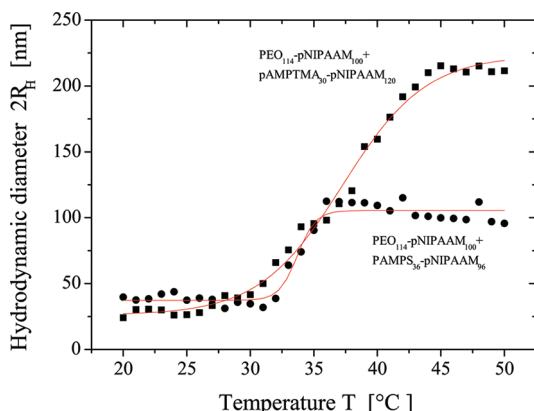


Figure 2. Hydrodynamic diameter $2R_H$ of PEO₁₁₄-*b*-PNIPAAm₁₀₀ + PAMPTMA₃₀-*b*-PNIPAAm₁₂₀ (upper curve) and PEO₁₁₄-*b*-PNIPAAm₁₀₀ + PAMPS₃₆-*b*-PNIPAAm₉₆ (bottom curve) as a function of temperature. The formation of micelles (or of other differently structured aggregates) occurs at the temperature of 36 °C, marked by the rapid increase of the aggregate size.

As can be seen, upon heating to 32 °C, the hydrodynamic diameter $2R_H$ sharply increased to approximately 100 nm, for PEO₁₁₄-*b*-PNIPAAm₁₀₀ + PAMPS₃₆-*b*-PNIPAAm₉₆ and up to about 200 nm for PEO₁₁₄-*b*-PNIPAAm₁₀₀ + PAMPTMA₃₀-*b*-PNIPAAm₁₂₀. These different sizes are a first print for a possible different structural arrangement induced by the temperature in these two polymeric systems. While in the former case the size is consistent with the one expected for micelles, in the latter case, because of the larger size, a more organized structure such as a vesicular structure can be hypothesized.

2.2.2. ζ -Potential Measurement. The electrophoretic mobility of polymeric particle aggregates was measured by means of laser microelectrophoresis technique, in a temperature-controlled cell (in the temperature interval from $T = 20$ to 50 °C, within the uncertainty of ± 0.2 °C) using a Malvern Zetasizer Mod. NanoZeta instrument (Malvern, U.K.). Since the particle size is much larger than the Debye screening length, the ζ -potential was calculated from the measured electrophoretic mobility u , by means of the Smolukovsky equation

$$\zeta = \frac{3\eta u}{2\epsilon_0 \epsilon_m f(k_D R)} \quad (3)$$

where η and ϵ_m are the viscosity and permittivity of the aqueous phase, ϵ_0 is the dielectric constant of free space, and $f(k_D R)$ is the Henry function,³¹ which depends upon the inverse of the Debye screening length k_D and the particle radius R . For $R \gg k_D^{-1}$, valid for relatively large particles in a medium of moderate

to high ionic strength, the Smoluchowski limit applies and $f(k_D R) = 1.5$.

The ζ -potential of PEO₁₁₄-*b*-PNIPAAm₁₀₀ + PAMPTMA₃₀-*b*-PNIPAAm₁₂₀ and PEO₁₁₄-*b*-PNIPAAm₁₀₀ + PAMPS₃₆-*b*-PNIPAAm₉₆ in aqueous suspension is shown in Figure 3, in

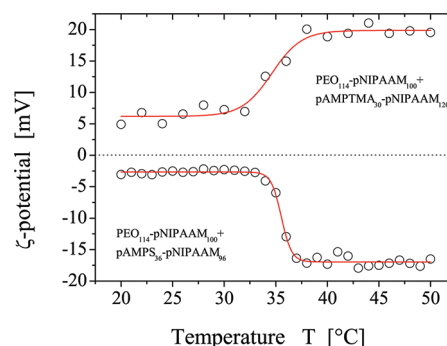


Figure 3. ζ -potential of PEO₁₁₄-*b*-PNIPAAm₁₀₀ + PAMPTMA₃₀-*b*-PNIPAAm₁₂₀ (upper curve) and PEO₁₁₄-*b*-PNIPAAm₁₀₀ + PAMPS₃₆-*b*-PNIPAAm₉₆ as a function of temperature (bottom curve). The formation of micelles (or of other differently structured aggregates) occurs at the temperature of 36 °C, marked by the rapid increase of the ζ -potential.

the whole temperature range investigated, from 10 to 50 °C. As can be seen, in correspondence of the lower critical solution temperature (LCST) at around 33–35 °C, ζ -potential increases toward higher values, positive or negative according to the ionization characteristic of the polyelectrolyte chain (PAMPS and PAMPTMA polyions, respectively), suggesting that structural rearrangement occurred. Moreover, at temperatures higher than LCST, ζ -potential keeps a constant value, indicating that thermally stable structures persist up to 50 °C.

The surface charge of the particles is calculated from the ζ -potential through the Ohshima relationship²⁵

$$\zeta = \frac{K_B T}{ze} \ln \left(\frac{1}{6\Phi \ln(1/\Phi)} \left(\frac{ze}{K_B T} \right)^2 \left(\frac{Q}{4\pi\epsilon_0 \epsilon_R R_H} \right)^2 \right) \quad (4)$$

where Φ is the volume fraction of the particles, (ze) the elementary charge, Qe the total electric charge over each particle, and R_H its radius. We obtained values of the order of $Q = 45$ elementary charges for the PEO₁₁₄-*b*-PNIPAAm₁₀₀ + PAMPTMA₃₀-*b*-PNIPAAm₁₂₀ system and $Q = 38$ for the PEO₁₁₄-*b*-PNIPAAm₁₀₀ + PAMPS₃₆-*b*-NIPAAm₉₆ system.

2.2.3. Dielectric Measurements. The dielectric and conductometric spectra of PAMPS₃₆-*b*-PNIPAAm₉₆ and PAMPTMA₃₀-*b*-PNIPAAm₁₂₀ polymers interacting with PEO₁₁₄-*b*-PNIPAAm₁₀₀ polymers in aqueous solutions at different temperatures have been measured in the frequency range from 1 kHz to 2 GHz by means of two radio frequency impedance analyzers, Hewlett-Packard model 4294A (in the frequency range from 1 kHz to 10 MHz) and model 4291A (in the frequency range from 1 MHz to 2 GHz). Details of the dielectric cell and the calibration procedure have been reported elsewhere.^{26–28}

3. ANALYSIS OF THE DIELECTRIC SPECTRA

The whole dielectric spectra of the aqueous polymer solutions have been described on the basis of a Cole–Cole relaxation function²⁹ modified by adding a further Debye relaxation to

take into account the contribution of the dielectric response at higher frequencies (orientational polarization of the aqueous phase) and by adding the contribution of a constant-phase-angle (CPA) element to take into account the contribution of the electrode polarization at lower frequencies.^{30,31} The whole relaxation function reads

$$\begin{aligned}\epsilon^*(\omega) &= \epsilon'(\omega) - i\epsilon''_{\text{tot}}(\omega) \\ &= A(i\omega)^{-\alpha} + \epsilon_{\infty} + \frac{\Delta\epsilon}{1 + (i\omega\tau)^{\beta}} + \frac{\Delta\epsilon_W}{1 + i\omega\tau_W} \\ &\quad + \frac{\sigma_0}{i\omega\epsilon_0}\end{aligned}\quad (5)$$

where the first term takes into account the scaling law that describes the electrode polarization effect and $\Delta\epsilon$, $\nu = 1/2\pi\tau$, and β are the dielectric increment, the relaxation frequency, and the spread parameter, respectively, of the dielectric relaxation process of interest here. $\Delta\epsilon_W$ and τ_W are the dielectric increment and the relaxation time of the aqueous phase and σ_0 the dc electrical conductivity. In this case, the dc electrical conductivity has been measured at a frequency of 1 kHz, well below the frequencies where the relaxation with which we are dealing occurs.

The details of the fitting procedure by which it is possible to extract the dielectric parameters of interest here have been described in detail elsewhere,³² and we invite the reader to refer to this reference. Here, we stress only that the deconvolution of the spectra has been carried out considering simultaneously the real $\epsilon'(\omega)$ and the imaginary $\epsilon''(\omega)$ parts of the complex dielectric constant $\epsilon^*(\omega)$ on the basis of the Levenberg–Marquardt algorithm for complex functions. The accuracy of the whole fitting procedure is within 1% for $\epsilon'(\omega)$ and within 1–2% for $\epsilon''(\omega)$.

4. RESULTS AND DISCUSSION

Typical dielectric spectra of PEO₁₁₄-*b*-PNIPAAm₁₀₀ + PAMPTMA₃₀ + *b*-PNIPAAm₁₂₀ polymer aqueous solutions at two selected temperatures (10 and 50 °C) are shown in Figure 4. The dielectric behavior of PEO₁₁₄-*b*-PNIPAAm₁₀₀ + PAMPS₃₆-*b*-PNIPAAm₉₆ polymer aqueous solution at the two above stated temperatures is shown in Figure 5.

Both the systems investigated present a very similar dielectric behavior, characterized by a marked dielectric dispersion falling at frequencies of the order of some hundreds of kilohertz in the first case and of the order of some megahertz in the second case, followed by a further dielectric relaxation due to the orientational polarization of the aqueous phase, whose maximum falls at frequencies well above the frequency window considered here. This latter dielectric response is well evidenced by the increase shown by the total dielectric loss in the high-frequency tail (see inset of Figure 5). In spite of the overall similar behavior, the temperature dependence of the dielectric parameters of the two polymeric systems presents some interesting features indicating again that different structural reorganizations induced by the temperature take place.

The dielectric parameters, i.e., the dielectric increment $\Delta\epsilon$, the relaxation frequency $\nu = 1/(2\pi\tau)$, and the Cole–Cole parameter β for the two polymer systems investigated, have been obtained by fitting eq 5 to the experimental results by means of the Levenberg–Marquardt algorithm for complex functions. In this way, the same set of the dielectric parameters

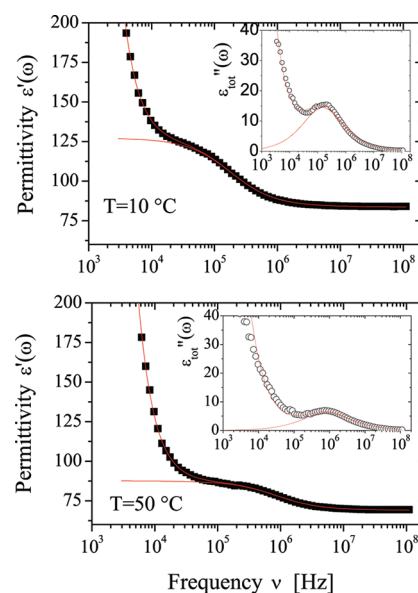


Figure 4. Dielectric spectra of PEO₁₁₄-*b*-PNIPAAm₁₀₀ + PAMPTMA₃₀-*b*-PNIPAAm₁₂₀ aqueous polymer solutions (polymer concentration $C = 5$ mg/mL) at two selected temperatures, 10 °C, upper panel, and 50 °C, bottom panel. The insets show the total dielectric loss $\epsilon''_{\text{tot}}(\omega)$. The full lines are the calculated values according to the relaxation function, eq 5.

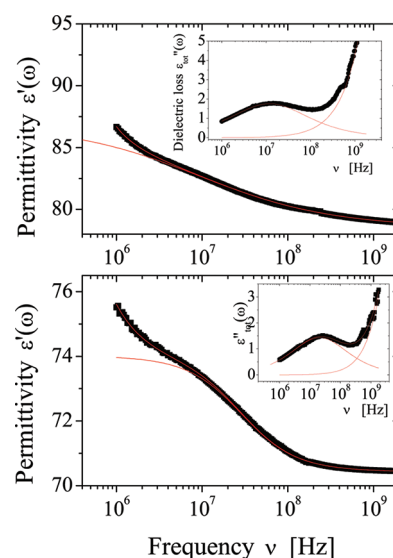


Figure 5. Dielectric spectra of PEO₁₁₄-*b*-PNIPAAm₁₀₀ + PAMPS₃₆-*b*-PNIPAAm₉₆ aqueous polymer solutions (polymer concentration $C = 5$ mg/mL) at two selected temperatures, 10 °C, upper panel, and 50 °C bottom panel. The insets show the total dielectric loss $\epsilon''_{\text{tot}}(\omega)$. The full lines are the calculated values according to the relaxation function, eq 5.

accounts for both the real and the complex parts of the complex dielectric constant $\epsilon^*(\omega)$. This procedure provides a good reliability of the results and, overall, ensures that the Kramer–Krönig relationship holds.

The results of this analysis are shown in Figure 6. As can be seen, close to the LCST, the slope of the temperature dependence of the dielectric increment $\Delta\epsilon$ and the relaxation frequency ν changes, indicating that a structural rearrangement of the polymer chains takes place. In particular, we observe that the dielectric relaxation falls in the range 10–30 MHz in the

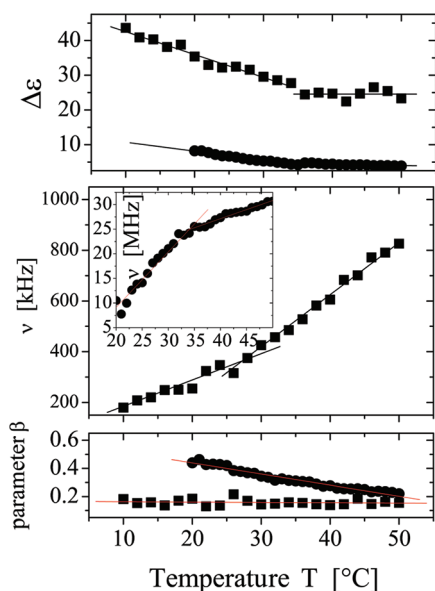


Figure 6. Dielectric parameters $\Delta\epsilon$ (upper panel), ν (intermediate panel), and β (bottom panel) of $\text{PEO}_{114}\text{-}b\text{-PNIPAAm}_{100}$ + $\text{PAMPS}_{36}\text{-}b\text{-PNIPAAm}_{96}$ aqueous polymer solutions (●) and of $\text{PEO}_{114}\text{-}b\text{-PNIPAAm}_{100}$ + $\text{PAMPTMA}_{30}\text{-}b\text{-PNIPAAm}_{120}$ (■) as a function of temperature, deduced from the fitting procedure of eq 5 to the experimental dielectric spectra. Polymer concentration $C = 5$ mg/mL.

case of $\text{PEO}_{114}\text{-}b\text{-PNIPAAm}_{100}$ + $\text{PAMPS}_{36}\text{-}b\text{-PNIPAAm}_{96}$ and in the range of 100–700 kHz in the case of $\text{PEO}_{114}\text{-}b\text{-PNIPAAm}_{100}$ + $\text{PAMPTMA}_{30}\text{-}b\text{-PNIPAAm}_{120}$ polymer solutions. This means that we are dealing with structures of basically different sizes, i.e., smaller aggregates in the former case and larger aggregates in the latter case. These features are also substantiated by results of dynamic light scattering measurements that have evidenced, above the LCST, for the two samples investigated, structures of 100 and 200 nm in size, respectively.

Before proceeding further in the analysis of the dielectric spectra, we want to give a quick look at the size of the two copolymers bearing the thermoresponsive block PNIPAAm. Below the LCST, the block copolymers should be molecularly dissolved in solution (unimers), with an *apparent* hydrodynamic radius of the order of 10 nm. Above the LCST, in the case of $\text{PAMPS}_{36}\text{-}b\text{-PNIPAAm}_{96}$ copolymers, the hydrodynamic diameter of the aggregate is more or less about 70 nm, i.e., around twice the value of the length of the fully stretched chain (assuming a monomer length of 0.25 nm). This value is fully compatible with the formation of core–shell micelles, where block copolymers are in their fully stretched conformation.¹⁸ In the case of $\text{PAMPTMA}_{30}\text{-}b\text{-PNIPAAm}_{120}$ copolymers, the value of the hydrodynamic diameter is about 47 nm, slightly lower than the value obtained for $\text{PAMPS}\text{-}b\text{-PNIPAAm}$ copolymers with the same ratio between the hydrophobic and hydrophilic block.¹⁹ These findings suggest that in the case of the basic copolymers we have investigated, both of them form aggregates that are largely compatible above the LCST with a micellar structure, the core of which is formed by PNIPAAm and the external shell is formed by PAMPTMA or, in turn, by PAMPS copolymers. The presence of the copolymers $\text{PEO}\text{-}b\text{-PNIPAAm}$ in $\text{PMPTMA}\text{-}b\text{-PNIPAAm}$ copolymers modifies this picture, giving rise to larger structures compatible with vesicles encompassing an aqueous core.

5. THE DIELECTRIC MODEL

Let us go back to the formation of mixed aggregates as the temperature increases over the LCST (≈ 35 °C).

Because we have experimentally observed from dynamic light scattering measurements, further confirmed by the relaxation frequencies of the dielectric dispersions, aggregates of different size with a relatively low polydispersity, we are induced to hypothesize two different dielectric models, respectively, for $\text{PEO}\text{-}b\text{-PNIPAAm}$ + $\text{PAMPS}\text{-}b\text{-PNIPAAm}$ and $\text{PEO}\text{-}b\text{-PNIPAAm}$ + $\text{PAMPTMA}\text{-}b\text{-PNIPAAm}$ polymer aqueous solutions.

In the former case, because of the smaller size (of the order of 100 nm), the micelle can be seen as built up by a spherical core formed by PNIPAAm polymers surrounded by a concentric shell of mixed PAMPS and PEO polymers.

In the latter case, with aggregates typically of 200 nm in size, we hypothesize a vesicular structure which encompasses an aqueous core surrounded by a concentric polymeric mixed shell composed by an inner hydrophobic layer (PNIPAAm polymers) and two adjacent hydrophilic layers (PEO and PAMPTMA polymers) bathing the internal and external aqueous phase.

These two different aggregation modalities are sketched in Figure 1. For each of them, we have adopted a different dielectric model, in the framework of the heterogeneous system effective medium approximation theory. In what follows, we will illustrate these models and will discuss some relevant consequences, as far as the characterization of these structures is concerned.

5.1. The Vesicle Model. In this case, as above stated, the aggregate consists of a polymeric composite layer formed by collapsed PNIPAAm polymers (the hydrophobic interior region) coated by a mixed corona of PEO and PAMPTMA polymers (the hydrophilic regions extending toward the exterior at both sides of the structure).

This closed layer, encompassing an aqueous core, represents the polymeric vesicle. This structure is made even more intricate by the presence of a positive charge distribution at the inner and outer interfaces, due to the (partial) ionization of the $^+\text{N}(\text{CH}_3)_3$ groups, with the release of Cl^- counterions in the aqueous phase.

This structure can be conveniently accounted for, at least from a dielectric point of view, by a model recently developed by Prodan et al.¹⁷ and further analyzed by one of us³³ in order to extend its validity to high values of the electrical conductivity of the shell layer. This model is particularly suitable to take into account the dielectric (and conductometric) properties of biological cell suspensions.¹⁷ The main merit of the model is the introduction of two surface charge distributions at the membrane interface that greatly influence the dielectric response of the whole system.

According to this model, each vesicle is represented by an aqueous core of complex dielectric constant $\epsilon_p^*(\omega) = \epsilon_p + \sigma_p/(\omega\epsilon_0)$, covered by a concentric region characterized by a complex dielectric constant $\epsilon_s^*(\omega) = \epsilon_s + \sigma_s/(\omega\epsilon_0)$ and randomly dispersed in a continuous medium of complex dielectric constant $\epsilon_m^*(\omega) = \epsilon_m + \sigma_m/(\omega\epsilon_0)$. Here, ϵ_j and σ_j ($j = p, s, m$) are the permittivity and the electrical conductivity of the three adjacent media, respectively. At each of the two aqueous interfaces, at the inner and outer interfaces, a surface charge distribution ρ exists.

It must be noted, however, that the intermediate region should reveal a composite structure built up by an inner

hydrophobic layer composed by PNIPAAm polymers, covered, at both sides, by a hydrophilic mixture of PEO and PAMPTMA polymers. A more rigorous dielectric characterization of the system should require an appropriate complex dielectric constant for each polymer component, resulting, however, in an excessive number of dielectric parameters to be easily handled. Because the permittivity of the two polymer does not differ too much,³⁴ we have assumed that this composite structure could be treated by the *average* complex dielectric constant $\epsilon_s^*(\omega)$, independent, to a first approximation, of the temperature.

Under the above stated scheme, within the framework of the Prodan model,¹⁷ and in the light of this approximation, the potential outside the shelled vesicle can be written as

$$\Psi(r, \vartheta) = -rE_0 \cos \vartheta + \left[p_1 + p_2 \left(\frac{R_2}{R_1} \right) \right] \frac{R_1^3}{r^2} \cos \vartheta \quad (6)$$

where the coefficients p_1 and p_2 are given by

$$p_1 = \frac{C - B}{AC - B} \quad (7)$$

$$p_2 = \frac{A - 1}{AC - B} \quad (8)$$

with

$$A = \frac{1 + \frac{D_1}{2R_1\gamma_1}(\epsilon_s^* + 2\epsilon_m^*)}{1 + \frac{D_1}{2R_1\gamma_1}(\epsilon_s^* - \epsilon_m^*)} \quad (9)$$

$$B = \frac{R_1}{R_2} \frac{1 - 2\frac{D_1}{2R_1\gamma_1}(\epsilon_s^* - \epsilon_m^*)}{1 + \frac{D_1}{2R_1\gamma_1}(\epsilon_s^* - \epsilon_m^*)} \quad (10)$$

$$C = \frac{R_1^2}{R_2^2} \frac{1 + \frac{D_2}{2R_2\gamma_2}(\epsilon_p^* + 2\epsilon_s^*)}{1 + \frac{D_2}{2R_2\gamma_2}(\epsilon_p^* - \epsilon_s^*)} \quad (11)$$

Here, $R_1 = R_2 + d$ and R_2 are the radius of the external and internal concentric spheres, with d the thickness of the shell. The quantities D_j ($j = 1, 2$) are defined as $D_j = 2D_j + i\omega R_j^2$, where D_j and γ_j are the diffusion coefficients and the conductivities of the charges at the two interfaces. The polarizability $\alpha(\omega)$ can be deduced from the dipolar term of the expansion of the potential $\Psi(r, \vartheta)$ outside the particle,³³ according to the relationship

$$\alpha(\omega) = 3 \left[p_1 + p_2 \left(\frac{R_2}{R_1} \right) \right] \quad (12)$$

and, finally, the complex dielectric constant $\epsilon^*(\omega)$ of the vesicle suspension can be written, in light of the effective medium approximation theory³⁵ as

$$\epsilon^*(\omega) = \epsilon_m^* \left[1 + \frac{\Phi \alpha(\omega)}{1 - \frac{1}{3} \Phi \alpha(\omega)} \right] \quad (13)$$

Equation 13 furnishes the full dielectric behavior of the polymer aqueous solution. We will limit our analysis to the main dielectric parameters of the dispersion, i.e., the dielectric increment $\Delta\epsilon$ and the relaxation frequency ν .

The above stated model mainly depends on two parameters, the diffusion coefficient D and the surface conductivity γ . These parameters control the strength of the dielectric dispersion (the dielectric increment $\Delta\epsilon$) and the relaxation frequency ν . Typical examples of the dielectric relaxations described by this model are shown in Figure 7, for different values of the

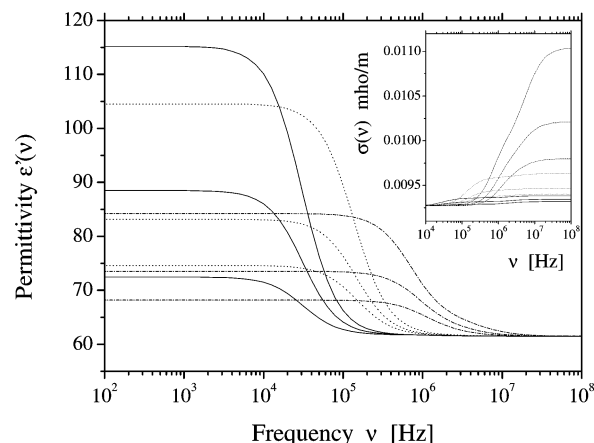


Figure 7. Typical dielectric relaxations derived from eq 13, for different values of the dielectric parameters. Full lines: $D_1 = D_2 = 10^{-9} \text{ m}^2/\text{s}$ and $\gamma_1 = \gamma_2 = 5.0, 2.5, 1.0 \text{ C}/(\text{V s})$ from top to bottom, respectively; dotted lines: $D_1 = D_2 = 5 \times 10^{-9} \text{ m}^2/\text{s}$ and $\gamma_1 = \gamma_2 = 20.0, 10.0, 5.0 \text{ C}/(\text{V s})$ from top to bottom, respectively; dashed lines: $D_1 = D_2 = 5 \times 10^{-8} \text{ m}^2/\text{s}$ and $\gamma_1 = \gamma_2 = 100, 50, 30 \text{ C}/(\text{V s})$ from top to bottom, respectively. The inset shows the corresponding behavior of the electrical conductivity $\sigma(\omega)$. The values of the dielectric phase parameters are $\epsilon_m = 65$, $\sigma_m = 10^{-2} \text{ mho/m}$; $\epsilon_p = 65$, $\sigma_p = 10^{-2} \text{ mho/m}$; $\epsilon_s = 10$, $\sigma_s = 10^{-5} \text{ mho/m}$; $R_1 = 100 \text{ nm}$; $R_2 = 50 \text{ nm}$. The fractional volume is $\Phi = 0.05$.

diffusion coefficient D and the surface conductivity γ , in the range of values of interest here. As can be seen, both the dielectric increment $\Delta\epsilon$ and the relaxation frequency ν can be conveniently tuned by means of appropriate values of the parameters.

The values of $\Delta\epsilon$ and ν calculated in the framework of this model have been compared with the ones obtained from the fitting procedure of eq 5 to the experimental spectra in Figure 8. Comparison has been carried out considering for the dielectric phase parameters of the aqueous phase ($\epsilon_m = \epsilon_p$ and $\sigma_m = \sigma_p$) the values measured at the temperature of the experiment and assuming for the polymeric shell of the vesicle the values $\epsilon_s = 10$ and $\sigma_s = 10^{-5} \text{ mho/m}$, both of them independent of temperature. The results are shown in Figure 8 for both the dielectric increment (upper panel) and the relaxation frequency (bottom panel), considering a diffusion coefficient $D_1 = D_2 = 1.3 \times 10^{-9} \text{ m}^2/\text{s}$ (corresponding to Na^+ ions at $T = 25^\circ \text{C}$) and a surface conductivity $\gamma_1 = \gamma_2 = 3.0 \text{ C}/(\text{V s})$. As can be seen, the whole agreement is quite good.

Two further comments are in order. First, we observe a dielectric increment $\Delta\epsilon$ independent of temperature, despite the fact that ϵ_m (and hence ϵ_p) decreases with the increase of the temperature. This interesting feature is justified by the behavior of the radius of the aggregates that continuously increases even above the LCST as observed by dynamic light

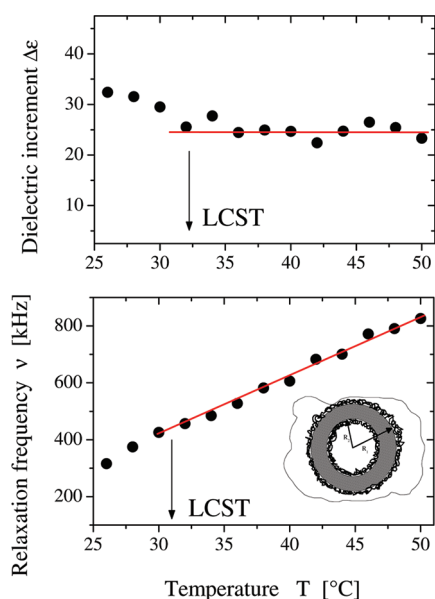


Figure 8. Dielectric increment $\Delta\epsilon$ (upper panel) and the relaxation frequency ν (bottom panel) of PEO₁₁₄-*b*-PNIPAAm₁₀₀ + PAMPTMA₃₀-*b*-PNIPAAm₁₂₀ polymer solutions at temperatures higher than the LCST compared with the corresponding values calculated on the basis of the Prodan model (eq 13). The inset shows the hypothesized vesicular structure.

scattering measurement (Figure 2). The model takes correctly into account these two opposite behaviors. Second, eq 13 does not give explicitly in closed form the expression of the relaxation frequency but furnishes the whole spectrum. We have described this spectrum by a single Debye relaxation function, and we have found the appropriate relaxation frequency ν and compared this value to the one experimentally derived from the analysis of the dielectric spectra.

From the above analysis, we can conclude that the proposed model is appropriate enough to describe the main features of the dielectric dispersion of an aqueous suspension of spherical vesicles bearing an electric charge distribution at both their aqueous interfaces.

5.2. The Micelle Model. In the case of PEO-*b*-PNIPAAm + PAMPS-*b*-PNIPAAm polymer solutions, the size of the aggregate (about 100 nm) at temperatures higher than the LCST is more or less twice the value of the contour length of fully stretched chains, and therefore this value is compatible with the formation of core-shell micelles, where the block copolymers are in their fully stretched conformation. Further evidence derives from the observed dielectric relaxation that falls at relatively high frequencies (of the order of some tens of megahertz, in comparison with the frequency relaxation of the order of 500 kHz, typical of PEO-*b*-PNIPAAm + PAMPTMA-*b*-PNIPAAm polymer solutions).

In the frequency window where the dielectric relaxation occurs (1 MHz–2 GHz), the dielectric behavior of the charged micelles in aqueous solution can be described, once the electrode polarization effects have been removed from the dielectric spectrum,^{30,31} within the framework of the standard electrokinetic model, extended, if necessary, to take into account the interfacial polarization of the Maxwell–Wagner effect.

Because of the ionization of the SO₃[−]Na⁺ groups of the PAMPS polymer, each micelle acquires a negative charge and,

simultaneously, a corresponding amount of Na⁺ ions are released in the bulk aqueous phase, giving rise to an ionic double layer at the particle aqueous interface.

Under the influence of an external electric field, an asymmetric charge distribution appears, producing an apparent dipole moment, whose relaxation is ultimately responsible for the observed dispersion in the frequency interval investigated.

This phenomenology is common to most parts of charged colloidal particle aqueous suspensions, and the dielectric interpretation has been well established in light of the standard electrokinetic model, in a series of works by Shilov, Grosse, and Dukhin and their co-workers.^{36–40}

In the present case, the overall dielectric response of PEO-*b*-PNIPAAm + PAMPS-*b*-PNIPAAm polymer solutions has been described, ignoring the Maxwell–Wagner dispersion effect because of its negligible contribution due to the relatively high ionic concentration, by a complex dielectric constant $\epsilon^*(\omega)$ ^{38,39} given by

$$\epsilon^*(\omega) = \epsilon_\infty + \Delta\epsilon f(\omega, \nu) + \frac{\sigma_0}{i\omega\epsilon_0} \quad (14)$$

where $\Delta\epsilon$ is the dielectric increment of the relaxation falling at the relaxation frequency ν . ϵ_∞ is the high-frequency limit of the permittivity, σ_0 the dc electrical conductivity, ω the angular frequency of the applied electric field, and ϵ_0 the dielectric constant of free space.

Disregarding the dependence on frequency and considering only the dielectric parameters, i.e., the total dielectric increment $\Delta\epsilon$, and the relaxation frequency ν , for a suspension of charged particles of average radius R_H with a fractional volume Φ , these two quantities are given by

$$\Delta\epsilon = \frac{9}{4}\Phi\epsilon_m(K_D R_H)^2 \frac{(S^+ - S^-)^2}{(S^+ + 2)^2(S^- + 2)^2} \quad (15)$$

$$\nu = \frac{D}{\pi R_H^2} \quad (16)$$

where $K_D = (\sigma_m/(D\epsilon_0\epsilon_m))^{1/2}$ is the inverse of the Debye screening length and the quantity S^\pm is defined by

$$S^\pm = \frac{4}{K_D R_H} \left(\exp \left[\mp \frac{ze\zeta}{2k_B T} \right] \right) \quad (17)$$

with D the counterion diffusion coefficient and ζ the ζ -potential.

As can be seen, the expected relaxation frequency ν (eq 16) depends only on the particle radius R_H and on the counterion diffusion coefficient D . Assuming a diffusion coefficient $D = 1.3 \times 10^{-9} \text{ m}^2/\text{s}$ (Na⁺, at $T = 25^\circ\text{C}$) with a temperature increment coefficient equal to $dD/dT = 0.0495 \times 10^{-9} \text{ m}^2/\text{s } ^\circ\text{C}$ and considering the value of the average radius R_H measured by means of DLS, eq 16 allows us to evaluate the relaxation frequency ν . As can be seen in Figure 9 (bottom panel), these values are in very good agreement with the ones experimentally observed, over the whole temperature interval higher than the LCST, where the polymers collapse into a micellar structure, showing that the temperature dependence of ν is completely justified by the analogous dependence of the diffusion coefficient D on the temperature.

The dielectric increment $\Delta\epsilon$ (eq 15) contains only a free adjustable parameter, the ζ -potential, that is, in the present case, experimentally accessible, through electrophoretic mobi-

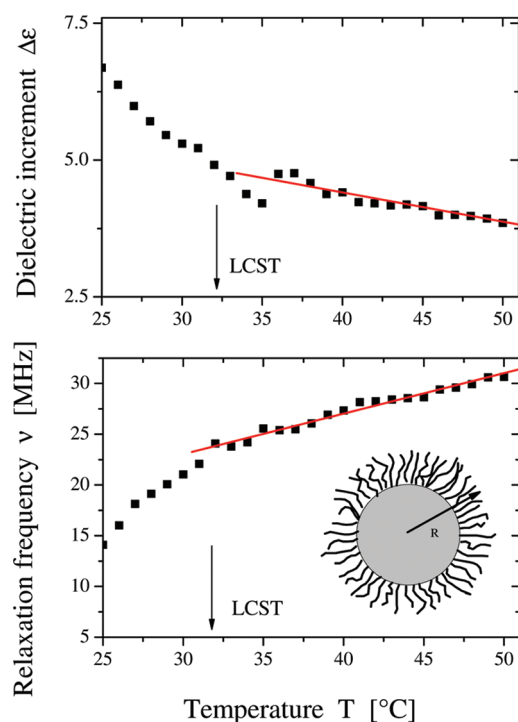


Figure 9. Dielectric increment $\Delta\epsilon$ (upper panel) and the relaxation frequency ν (bottom panel) of PEO_{114} - b -PNIPAAm₁₀₀ + PAMPS_{36} - b -PNIPAAm₉₆ polymer solutions at temperatures higher than the LCST compared with the corresponding values calculated on the basis of eqs 15 and 16. The inset shows the hypothesized micellar structure.

lity measurements. We have obtained, at temperatures higher than the LCST, values of ζ -potential of -17.5 mV, largely independent of temperature (Figure 3). Figure 9, upper panel, shows the dielectric increment $\Delta\epsilon$ together with the values calculated on the basis of eq 15, considering the measured values of the average size R_{H} and of the ζ -potential. As can be seen, the agreement is quite good and, also in this case, the dependence on the temperature is taken into account by the decrease of the permittivity of the aqueous phase ϵ_{m} as the temperature increases. As above stated, the ζ -potential is largely independent of the temperature (as confirmed experimentally (Figure 3)), suggesting that the surface charge density at the particle surface does not vary with temperature changes.

6. MORE ON THE DIELECTRIC MODELS

In order to further validate the choice of the dielectric models employed, we have considered the possibility of describing PEO - b -PNIPAAm + PAMPTMA - b -PNIPAAm polymer solutions in light of a micellar structure (instead of a vesicular structure) and conversely PEO - b -PNIPAAm + PAMPS - b -PNIPAAm polymer solution in light of a vesicular structure (instead of a micellar structure).

The experimental findings against the first hypothesis are the hydrodynamic radius, too large to accommodate the hydrophobic PNIPAAm core and a mixed hydrophilic PEO + AMPS shell, and the relatively low relaxation frequency we have experimentally observed, that is indicative, whatsoever the dielectric model is, of larger size objects.

The same justifications can be put forward to contrast the second hypothesis, since in this case the hydrodynamic radius is too small because a vesicle can be built up and, moreover, the

relaxation frequency experimentally observed is relatively high, indicative of objects of smaller size.

Moreover, in the case of micellar structures, the maximum value of the dielectric increment $\Delta\epsilon$ allowed in light of the electrokinetic model (see eq 15), once the ζ -potential has been measured, is only few dielectric units, which is well below the one we have experimentally observed. This finding rules out the possibility that a micellar structure could account for the dielectric parameters observed in the case of the PEO - b -PNIPAAm + PAMPTMA - b -PNIPAAm polymer system.

A further comment is in order. In principle, if one should hypothesize a structure consisting of central core, where a fraction of PAMPTMA and PNIPAAm polymers coexist together with an external shell of PEO chains, further incongruence will appear. As a matter of fact, while the aggregate size could fit with the value observed from dynamic light scattering measurements, we expect a ζ -potential considerably lower than the one experimentally observed and as a consequence a reduced surface charge. On the contrary, the ζ -potential is of the order of 20 mV, compatible with a charge born by the totality of PAMPTMA polymer chains. These further remarks should be in favor of a vesicular structure, as we have proposed.

7. INFLUENCE OF PEO - b -PNIPAAm COPOLYMER ON THE AGGREGATION PROCESS

In this last section, we are dealing with the aggregation behavior of PAMPS_{36} - b -PNIPAAm₉₆ and of PAMPTMA_{30} - b -PNIPAAm₁₂₀ aqueous polymer solutions in the absence of PEO - b -PNIPAAm copolymer. The hydrodynamic diameter of the aggregates at temperatures higher than the LCST has been previously measured, and a value of 70 nm (at temperatures higher than 33 $^{\circ}\text{C}$) has been obtained in the first case¹⁸ and a value of 47 nm (at temperatures higher than 37 $^{\circ}\text{C}$) in the second case.¹⁹ In both the cases, if compared with the contour length of fully stretched chains calculated assuming a monomer contour length of $l = 0.25$ nm, the values of the hydrodynamic diameter revealed from dynamic light scattering are compatible with the formation of core-shell micelles.

Further suggestion to this view comes from the values of the ζ -potential we have measured in the two above stated situations (see Figure 10). As can be seen, once the aggregation occurred,

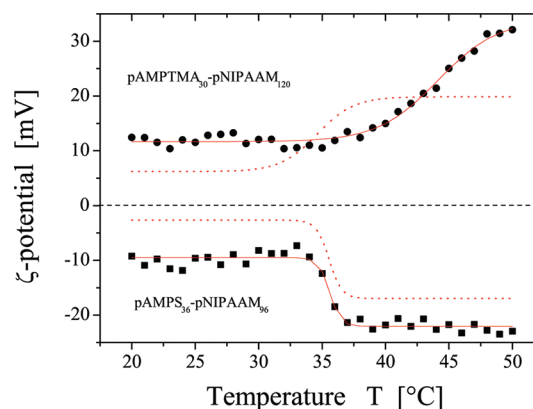


Figure 10. ζ -potential of PAMPS_{36} - b -PNIPAAm₉₆ aqueous polymer solutions (■) and of PAMPTMA_{30} - b -PNIPAAm₁₂₀ aqueous polymer solution (●) as a function of temperature. The dotted lines represent the value of the ζ -potential in the presence of PEO - b -PNIPAAm copolymer (fitted values from data of Figure 3).

ζ -potential is considerably higher than the corresponding values observed in the presence of PEO-*b*-PNIPAAm copolymers. This finding is justified by the different length of PEO ($n = 114$) and of ones of PAMPS and PAMPTMA polymers ($n = 36$ and $n = 30$, respectively). PEO chains exert a sort of charge shielding, reducing the effective surface charge bearing each particle.

Therefore, we are induced to assume that both the polymeric systems, being molecularly dissolved in solution (unimers) below the LCST with a hydrodynamic radius between 5 and 9 nm, collapse in a core-shell micellar structure at temperatures higher than the LCST, with size of the order of 47 and 70 nm, respectively. The presence of the PEO-*b*-PNIPAAm copolymer induces a different aggregation process, yielding a vesicular structure in the case of PEO-*b*-PNIPAAm + PAMPTMA-*b*-PNIPAAm copolymers.

8. CONCLUSIONS

The effect of temperature on the association behavior of two different thermoresponsive copolymers in aqueous solution has been investigated by means of dielectric relaxation spectroscopy measurements, together with dynamic light scattering and ζ -potential measurements. While PEO-*b*-PNIPAAm + PAMPS-*b*-PNIPAAm systems tend to self-assemble into micellelike structures, consisting of a hydrophilic corona and a hydrophobic core, the observed behavior of the PEO-*b*-PNIPAAm + PAMPTMA-*b*-PNIPAAm system suggests that, on the basis of an appropriate dielectric model, a vesicular structure is likely probable. Despite the similarity of the two systems investigated, as far as the chemical structure is concerned, the two systems behave differently, emphasizing the role of the delicate balance between repulsive electrostatic forces and hydrophobic interactions in the temperature-induced self-assembling. The different structures have been modeled, from a dielectric point of view, on the basis of two different dielectric models which emphasize their main features. In the case of a micellar structure, the main contribution arises from the counterion polarization in the neighborhood of the particle interface, and the dielectric phenomenology has been described in light of the standard electrokinetic model. In the case of the vesicular structure, the main characteristic is the presence of an aqueous core and the further presence of two thick distributed layers of electric charge at the two aqueous interfaces. We have taken advantage of a dielectric model recently proposed by Prodan et al.,¹⁷ specifically developed for biological spherical cells, and have shown how this model is appropriate enough to describe the dielectric phenomenology we have observed in these systems. The thermoresponsive properties of these polymers and the resulting self-assembled structures make them promising starting points for a variety of applications, particularly in the field of drug encapsulation and following drug delivery, and further studies are underway.

AUTHOR INFORMATION

Corresponding Author

*Fax +39 06 4463158; e-mail cesare.cametti@roma1.infn.it.

Notes

The authors declare no competing financial interest.

ACKNOWLEDGMENTS

The authors are indebted to the "Ministero dell'Università e della Ricerca Scientifica" (Italy) for financial support in the frame of the PRIN-2008.

REFERENCES

- (1) Cui, Q.; Wu, F.; Wang, E. *J. Phys. Chem. B* **2011**, *115*, 5913–5922.
- (2) Malaki, A.; Kjoniksen, A. L.; Zhu, K.; Nystrom, B. *J. Phys. Chem. B* **2011**, *115*, 8975–8982.
- (3) Schmidt, R. R.; Pamies, R.; Kjoniksen, A.-L.; Zhu, K.; Cifre, J. G. H.; Nystrom, B.; de la Torre, J. G. *J. Phys. Chem. B* **2010**, *114*, 8887–8893.
- (4) Jain, S.; Bates, F. S. *Science* **2003**, *300*, 460–464.
- (5) De, M.; Ghoo, P. S.; Rotello, V. M. *Adv. Mater.* **2008**, *20*, 4225–4241.
- (6) Ganta, S.; Devalapally, H.; Shahiwala, A.; Amiji, M. *Controlled Release* **2008**, *126*, 187–204.
- (7) Li, W.; Zhang, A.; Chen, Y.; Feldman, Y.; Wu, H.; Schlüter, D. A. *Chem. Commun.* **2008**, 5948–5950.
- (8) Inoue, K. *Prog. Polym. Sci.* **2000**, *25*, 453–571.
- (9) Irfan, M.; Seiler, M. *Ind. Eng. Chem. Res.* **2010**, *49*, 1169–1196.
- (10) Gao, H.; Matyjaszewski, K. *Prog. Polym. Sci.* **2009**, *34*, 317–350.
- (11) Hirokawa, Y.; Tanaka, T. *J. Phys. Chem.* **1984**, *81*, 6379–6384.
- (12) Schild, H. G. *Prog. Polym. Sci.* **1992**, *17*, 163–173.
- (13) Bae, Y. H.; Okano, T.; Kim, S. W. *J. Polym. Sci., Part B: Polym. Phys.* **1990**, *28*, 923–932.
- (14) Siband, E.; Trau, Y.; Hourdit, D. *Macromolecules* **2011**, *44*, 8185–8194.
- (15) *Block copolymers in Nanoscience*; Lazzari, M.; Liu, G.; Lecommandoux, S., Eds.; Wiley-VCH: Weinheim, Germany, 2006.
- (16) Masci, G.; De Santis, S.; Cametti, C. *J. Phys. Chem. B* **2011**, *115*, 2196–2204.
- (17) Prodan, E.; Prodan, C.; Miller, H. *Biophys. J.* **2008**, *95*, 4174–4182.
- (18) Masci, G.; Diociaiuti, M.; Crescenzi, V. *J. Polym. Sci., Part A: Polym. Chem.* **2008**, *46*, 4830–4842.
- (19) Patrizi, M. L.; Diociaiuti, M.; Capitani, D.; Masci, G. *Polymer* **2009**, *50*, 467–474.
- (20) De Santis, S.; Ladogana, R. D.; Diociaiuti, M.; Masci, G. *Macromolecules* **2010**, *43*, 1992–2001.
- (21) Masci, G.; Giacomelli, L.; Crescenzi, V. *Macromol. Rapid Commun.* **2004**, *25*, 559–564.
- (22) Berne, B. J.; Pecora, R. *Dynamic light scattering: Applications to chemistry, biology and physics*; Dover: New York, 2000.
- (23) Morrison, I.; Grabowski, E.; Herb, C. *Langmuir* **1985**, *1*, 469–501.
- (24) Provencher, S. W. *Comput. Phys. Commun.* **1982**, *27*, 213–219.
- (25) Ohshima, H. *J. Colloid Interface Sci.* **2002**, *247*, 18–23.
- (26) Masci, G.; Cametti, C. *J. Phys. Chem. B* **2009**, *113*, 11421–11428.
- (27) Cametti, C.; Fratoddi, I.; Venditti, I.; R. M., V. *Langmuir* **2011**, *27*, 7084–7090.
- (28) Bordini, F.; Cametti, C.; Motta, A.; Paradossi, G. *J. Phys. Chem. B* **1999**, *103*, 5092–5099.
- (29) Havriliak, S. J.; Havriliak, S. J. *Dielectric and mechanical relaxation in materials*; Hanser: New York, 1997.
- (30) Sanabria, H.; Miller, J. H. *J. Phys. Rev. E* **2006**, *74*, 051505.
- (31) Pizzitutti, F.; Bruni, F. *Rev. Sci. Instrum.* **2001**, *72*, 2502–2504.
- (32) Cametti, C.; Marchetti, S.; Gambi, C. M. C.; Onori, G. *J. Phys. Chem. B* **2011**, *115*, 7144–7153.
- (33) Di Biasio, A.; Cametti, C. *Phys. Rev. E* **2010**, *82*, 021917.
- (34) van Krevelen, D. W. *Properties of polymers*; Elsevier: The Netherlands, 1997.
- (35) Cametti, C. *Riv. Nuovo Cimento* **2009**, *32*, 185–260.
- (36) Grosse, C. In *Interfacial electrokinetics and electrophoresis*; Delgado, A. V., Ed.; Marcel Dekker, Inc.: New York, 2002; Vol. 106,

Chapter Relaxation mechanisms of homogeneous particles and cells suspended in aqueous electrolyte solutions, pp 277–327.

(37) Dukhin, S. S.; Shilov, V. N. In *Interfacial electrokinetics and electrophoresis*; Delgado, A. V., Ed.; Marcel Dekker, Inc.: New York, 2002; Vol. 106, Chapter Nonequilibrium electric surface phenomena and extended electrokinetic characterization of particles, pp 55–85.

(38) Grosse, C. *Interfacial electrokinetics and electrophoresis*; Delgado, A.V., Ed.; Marcel Dekker: New York, 2001.

(39) Grosse, C. *Encyclopedia of surface and colloid science*; Elsevier: New York, 2002.

(40) Delgado, A. V.; Arroyo, F. J. In *Interfacial electrokinetics and electrophoresis*; Delgado, A. V., Ed.; Marcel Dekker, Inc.: New York, 2002; Vol. 106, Chapter Electrokinetic phenomena and their experimental determination: An overview, pp 1–54.